Available online at www.sciencedirect.com

SCIENCE DIRECT®

Tectonophysics 391 (2004) 303–314

TECTONOPHYSICS

www.elsevier.com/locate/tecto

A study of microearthquake seismicity and focal mechanisms within the Sea of Marmara (NW Turkey) using ocean bottom seismometers (OBSs)

Toshinori Sato[a], Junzo Kasahara[b], Tuncay Taymaz[c,*], Masakazu Ito[b], Aya Kamimura[b,d], Tadaaki Hayakawa[b], Onur Tan[c]

[a]*Department of Earth Sciences, Faculty of Science, Chiba University, 1-33 Yayoi-cho, Inage-ku, Chiba 263-8522, Japan*
[b]*Earthquake Research Institute, University of Tokyo, 1-1-1 Yayoi, Bunkyo-ku, Tokyo 113-0032, Japan*
[c]*Seismology Section, Department of Geophysics, Faculty of Mines, Istanbul Technical University, Maslak, TR-34390, Istanbul, Turkey*
[d]*Now at National Institute for Earth Sciences and Disaster Prevention, 3-1 Tennodai, Tsukuba 305-0006, Japan*

Accepted 3 June 2004
Available online 27 September 2004

Abstract

We have carried out seismological observations within the Sea of Marmara (NW Turkey) in order to investigate the seismicity induced after Gölcük–İzmit (Kocaeli) earthquake (M_w 7.4) of August 17, 1999, using ocean bottom seismometers (OBSs). High-resolution hypocenters and focal mechanisms of microearthquakes have been investigated during this Marmara Sea OBS project involving deployment of 10 OBSs within the Çınarcık (eastern Marmara Sea) and Central-Tekirdağ (western Marmara Sea) basins during April–July 2000. Little was known about microearthquake activity and their source mechanisms in the Marmara Sea. We have detected numerous microearthquakes within the main basins of the Sea of Marmara along the imaged strands of the North Anatolian Fault (NAF). We obtained more than 350 well-constrained hypocenters and nine composite focal mechanisms during 70 days of observation. Microseismicity mainly occurred along the Main Marmara Fault (MMF) in the Marmara Sea. There are a few events along the Southern Shelf. Seismic activity along the Main Marmara Fault is quite high, and focal depth distribution was shallower than 20 km along the western part of this fault, and shallower than 15 km along its eastern part. From high-resolution relative relocation studies of some of the microearthquake clusters, we suggest that the western Main Marmara Fault is subvertical and the eastern Main Marmara Fault dips to south at ~45°. Composite focal mechanisms show a strike-slip regime on the western Main Marmara Fault and complex faulting (strike-slip and normal faulting) on the eastern Main Marmara Fault.

Keywords: Earthquakes; Fault mechanisms; Marmara sea; Ocean bottom seismology; Seismotectonics; Turkey

* Corresponding author. Tel.: +90 212 285 6245; fax: +90 212 285 6201.
E-mail addresses: taymaz@itu.edu.tr (T. Taymaz), satot@earth.s.chiba-u.ac.jp (T. Sato), ri2j_kshr@ybb.ne.jp (J. Kasahara).

0040-1951/$ - see front matter © 2004 Elsevier B.V. All rights reserved.
doi:10.1016/j.tecto.2004.07.018

1. Introduction

The Sea of Marmara is a marine basin in northwest Turkey, which connects the Aegean Sea with the Black Sea and includes a series of tectonically active basins, at the western end of the right-lateral North Anatolian Fault (NAF). It is 275 km long and 80 km wide, with a broad shallow shelf to the south and a series of deep (up to 1280 m) sub-basins to the north (Fig. 1). Across most of Turkey the NAF is a relatively simple, narrow, right-lateral strike-slip fault zone. However, it splits into several fault strands in the vicinity of the Sea of Marmara, so that the deformation becomes distributed over a 120-km-wide zone (Barka and Kadinsky-Cade, 1988; Taymaz et al., 1991; Smith et al., 1995; Taymaz, 1999; Okay et al., 2000; İmren et al., 2001; Le Pichon et al., 2001). The Marmara Sea is also a transition zone between the strike-slip regime of the NAF and the extensional regime of the Aegean Sea. The NAF bifurcates at the eastern end of the Marmara Sea. The main features of the NAF in the Sea of Marmara, the Main Marmara Fault (hereafter, MMF), has been imaged from a multibeam survey by IFREMER N/O Le Suroit (bathymetry in Fig. 1b, after Rangin et al., 2001, Le Pichon et al., 2001, Armijo et al., 2002). Le Pichon et al. (2001) described the MMF as a single localized active throughgoing right-lateral strike-slip fault segment. On the other hand, Armijo et al. (2002) reinterpreted it as having several oblique extensional segments separated by zones of distributed deformation.

The August 17, 1999, Gölcük–İzmit (Kocaeli) earthquake (M_w 7.4) ruptured the NAF at the eastern end of the Sea of Marmara (e.g., Taymaz, 1999, 2000; Taymaz et al., 2001, 2002; Özalaybey et al., 2002; Karabulut et al., 2002). Migration of seismicity westward along the NAFZ to this point, involving a series of large earthquakes, occurred earlier in the twentieth century. Historical records indicate that at least two events larger than M 7 occurred in the Sea of Marmara in the past 500 years (in 1509 and 1766), where no large earthquake occurred in the twentieth century (Ambraseys and Jackson, 2000). These facts suggest that the present probability of large earthquake occurrence in the Marmara Sea region is rather high. To assess this seismic hazard, it is also important to investigate fault geometry at depth. Le Pichon et al. (2001) conducted a high-resolution bathymetric, sparker and deep-towed seismic reflection survey, which revealed in detail the fault systems in the Sea of Marmara. Study of microseismicity study is also useful to investigate fault configurations on the scale of a few tens of kilometers. Before the present study, little was known about the microseismicity and microearthquake focal mechanisms in the Sea of Marmara. Land-based observations were recently conducted (Gürbüz et al., 2000), but these were insufficient to describe detailed fault geometries and microearthquake activity in the Sea of Marmara. This paper presents the results of the first marine seismological observations using ocean bottom seismometers (OBSs) in the Sea of Marmara to investigate its detailed microseismicity.

2. Observations and data acquisition

We conducted the Marmara Sea OBS project in two phases. We deployed 10 pop-up type OBSs (Kasahara et al., 1995) each time, during April 28–June 2, 2000 (Leg 1), and June 14–July 17, 2000 (Leg 2), in the eastern and western Sea of Marmara, respectively. The spacing of these OBSs was 10–20 km (Fig. 1b). The locations and observation periods of these OBSs are summarized in Table 1. The total observation period was 70 days. All OBSs were equipped with three-component velocity sensors, with 2 Hz natural frequency, and a digital recording system. Data was continuously recorded on magneto-optical disk. We determined the location of each OBS to within 20 m (one standard deviation) using acoustic measurements of distances between the OBS and the research vessel. All OBSs recorded good-quality data, but the clock calibration system of OBS-1 was out of order during Leg 1. We thus estimated the difference between true time and the internal time of OBS-1 using P-wave arrival time vs. S–P interval diagrams for microearthquakes. We added the estimation errors of this clock correction (about 200 ms) to each picking error for OBS-1.

To detect seismic events, we used an event picker algorithm based on the ratio between the short-term average and long-term average, and the duration of events (Sato et al., 1997). We then extracted the events that were recorded at four or more stations, and thus

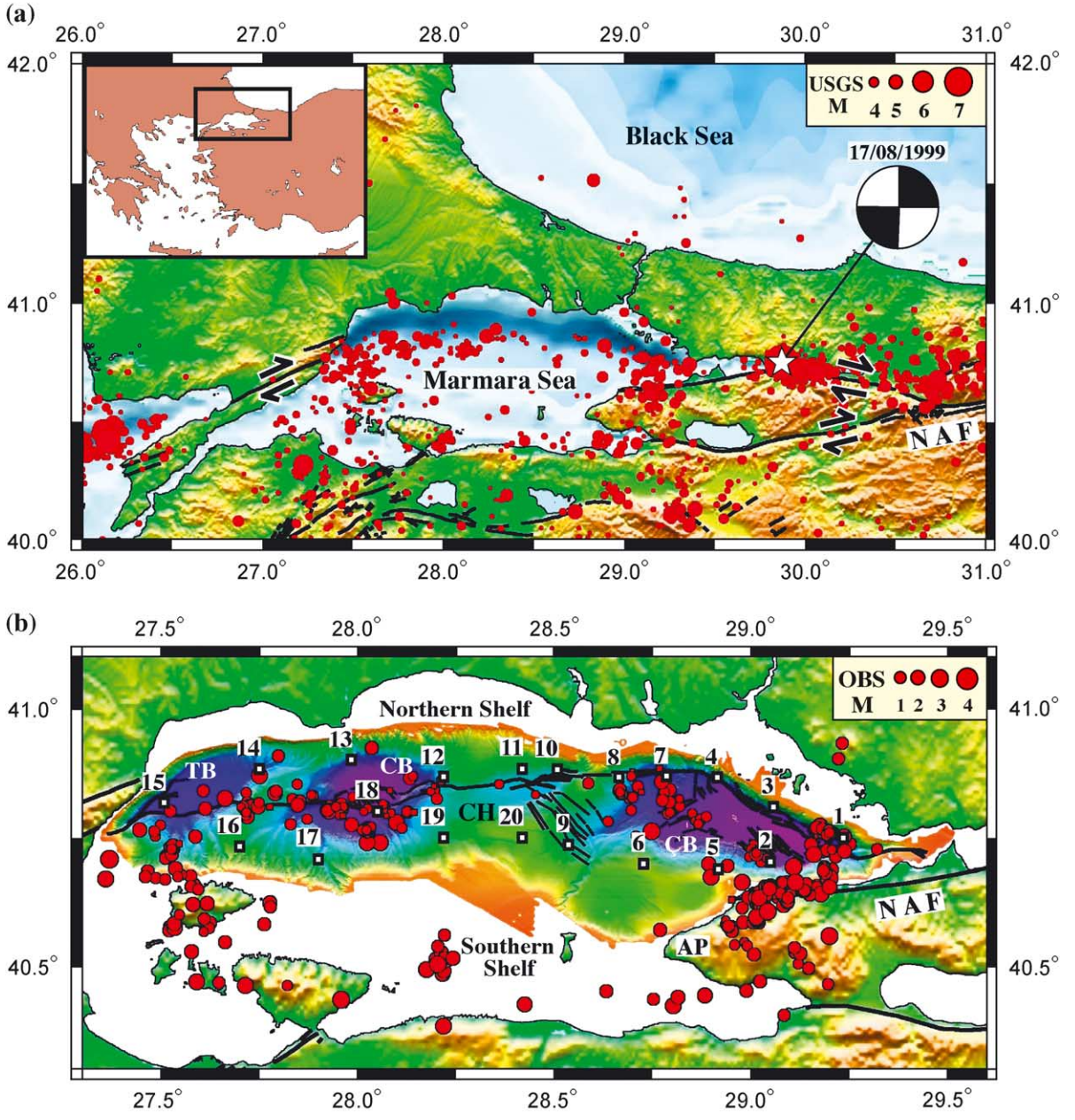

Fig. 1. (a) Seismicity of M>2 within the Marmara Region during 1996–2000. Data are from US Geological Survey (NEIS). Star indicates the epicenter of the 1999 Gölcük–İzmit (Kocaeli) earthquake, the focal mechanism for it being by Taymaz (1999). NAF indicates the North Anatolian Fault. Background is GTOPO-30 Global Topography Data, provided by the USGS-NIMA and resampled at 0.1-min resolution. Bathymetry data was provided by Smith and Sandwell (1997). (b) Distribution of microearthquake epicenters determined in this study. The standard error in each of the hypocentral coordinates is less than 5 km. The radius of each circle is proportional to magnitude. Squares with numbers indicate OBS locations. Tekirdağ Basin (TB), Central Basin (CB), Central High (CH), Çınarcık Basin (ÇB), Armutlu Peninsula (AP). Multibeam bathymetry data and interpretation of the Main Marmara Fault follow Le Pichon et al. (2001) and Rangin et al. (2001).

Table 1
Locations and operation periods of ocean bottom seismometers (OBSs)

OBS no.	Latitude (°N)	Longitude (°E)	Depth (m)	Operation period
1	40.7504	29.2327	842	28 April–2 June 2000
2	40.7034	29.0482	1105	28 April–2 June 2000
3	40.8082	29.0566	652	28 April–2 June 2000
4	40.8656	28.9127	963	28 April–2 June 2000
5	40.6894	28.9137	409	28 April–2 June 2000
6	40.6991	28.7250	308	28 April–2 June 2000
7	40.8676	28.7820	1050	28 April–2 June 2000
8	40.8671	28.6618	618	28 April–2 June 2000
9	40.7363	28.5326	584	28 April–2 June 2000
10	40.8808	28.5049	756	28 April–2 June 2000
11	40.8842	28.4164	579	14 June–17 July 2000
12	40.8674	28.2160	649	14 June–17 July 2000
13	40.8997	27.9829	912	14 June–17 July 2000
14	40.8835	27.7504	935	14 June–17 July 2000
15	40.8177	27.5079	1085	14 June–17 July 2000
16	40.7330	27.6990	440	14 June–17 July 2000
17	40.7091	27.9038	624	14 June–17 July 2000
18	40.7992	28.0494	1181	14 June–17 July 2000
19	40.7502	28.2158	525	14 June–17 July 2000
20	40.7503	28.4159	342	14 June–17 July 2000

made a common event list that includes over 2000 events. Because of contamination by ship traffic noise, we recognized by visual inspection that nearly half of these events were generated by such noise. Fig. 2 shows a typical example of an event acquired by these OBSs.

3. Hypocenter distribution in the Marmara Sea

We used the HYPOMH algorithm for hypocenter determination (Hirata and Matsu'ura, 1987) with the one-dimensional velocity model of Gürbüz et al. (2000) (Fig. 3). We calculated hypocenters with station corrections to compensate for errors caused by thickness variations in the sedimentary layer. These corrections were estimated using the interval between the P- and PS-phases (see Fig. 2), PS being converted from a P-wave to an S-wave at the boundary between sediment and crustal basement (Sato et al., 1999). The P-wave velocity V_p and the ratio of V_p/V_s for the sediment were assumed to be 2.0 km/s and 2.76, respectively, from other OBS surveys (Hirata et al., 1989). Residuals at each station were then averaged for all earthquakes. We added these averaged residuals to the station correction for each OBS in a second calculation. The magnitude M of each event was estimated using its total duration time T (s) and the relation

$$M = a + b\log_{10}T$$

(Tsumura, 1967). The OBSs also recorded three earthquakes whose magnitudes were also determined by the US Geological Survey. We estimated the coefficients a and b to be -4.30 and 3.54, respectively, from combined analyses of these three earthquakes.

During the observation period, we determined hypocenters of more than 350 events in the Marmara Sea region with error estimates of less than 5 km (Figs. 1b and 4). The observed hypocenter distribution shows that most of these microearthquakes occurred in the vicinity of the western MMF. In the eastern (Çınarcık) basin, on the other hand, fewer earthquakes occurred just beneath the MMF; they instead clustered to the south of the MMF (as defined by Le Pichon et al., 2001, which here follows the northern edge of the Çınarcık basin). The Central High had low microseismicity, and there were also few events along the southern shelf. However, a cluster was observed in the northern part of Armutlu Peninsula (Fig. 4).

We did not detect any earthquakes deeper than 20 km, but the observed depth distribution is mainly applicable for the Çınarcık, Central, and Tekirdağ basins. The depth distributions for the southern shelf

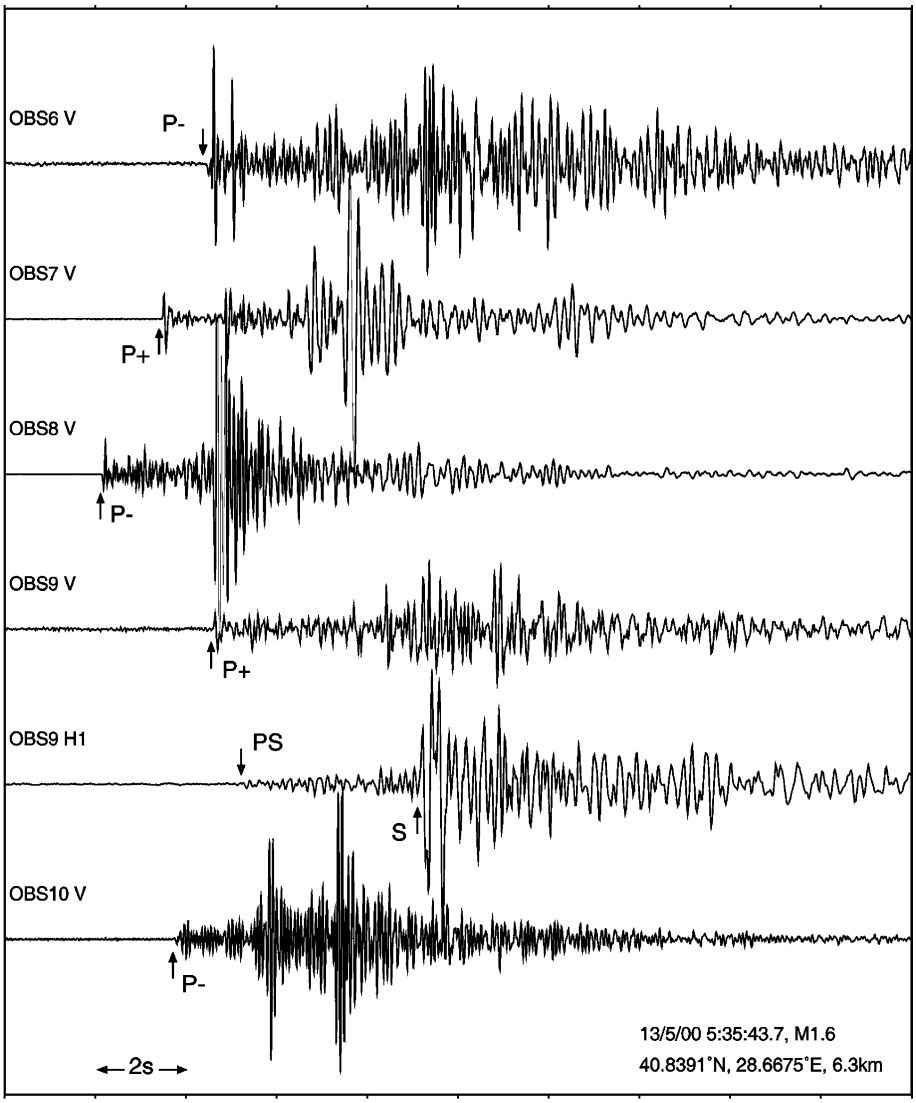

Fig. 2. Example seismograms recorded by OBSs for one microearthquake. V and H indicate vertical and horizontal components. P, S, and PS phases are indicated by arrows. Polarity of P phases is indicated by + and −.

and Armutlu Peninsula are not well constrained, because the events in these areas were located outside the OBS networks. The depth limit of events is 15 km in the eastern Sea of Marmara, but 20 km in its western part. No shallow events (depth <5 km) occurred along the MMF. The hypocenter distributions obtained from high-resolution relative relocations of clusters (see Section 4) suggest that the western MMF is sub-vertical, whereas the eastern MMF appears to dip steeply to the south.

4. High-resolution relative relocation of hypocenters

The different geometries of the western and eastern parts of the MMF were noted in the previous section. To investigate their microseismicity in detail, we relocated the hypocenters using a high-resolution relative relocation method, HypoDD (Waldhauser and Ellsworth, 2000), which is a useful tool for studying precise relative locations of events in a cluster. We

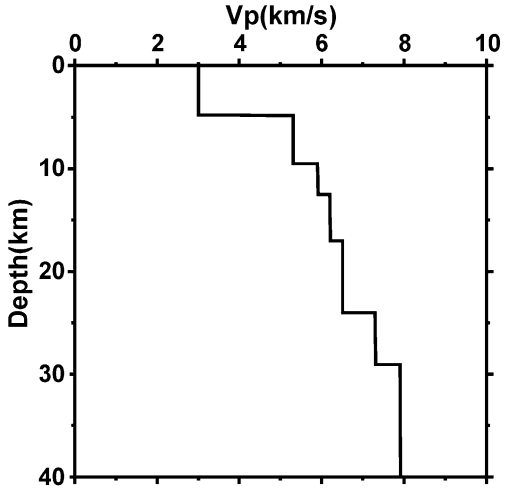

Fig. 3. Adopted model of P-wave velocity structure used for hypocenter determination (after Gürbüz et al., 2000).

selected three clusters: along the western MMF; in the western Çınarcık Basin; and at eastern end of the MMF, all located within the OBS network near the MMF (Fig. 5a). We used the HypoDD program (Waldhauser, 2001) with phase pick data, and set the maximum separation distance for all events in a cluster as 5 km. The mean location uncertainties of relocated events were ~200 m, the maximum being 990 m.

Fig. 5 shows the relocated hypocenters for the clusters along the western MMF (Fig. 5b), in the western Çınarcık Basin (Fig. 5c) and at the eastern end of the MMF (Fig. 5d). Along the western MMF, we can recognize that most earthquakes occurred just beneath the fault except the shallowest events that were located south of OBS 18. This suggests that the western MMF is subvertical. Le Pichon et al. (2001) and Armijo et al. (2002) reported a spindle-shaped structure in the Central Basin. Our results show that microearthquakes occurred only beneath its southern half, at depths of up to 20 km. This suggests that only southern half of the structure is relatively active, and the fault geometry is subvertical.

The N–S cross-section across the western Çınarcık Basin (Fig. 5c) indicates that the microearthquake distribution dips toward the south at ~45°. This indicates that the MMF is locally not vertical, but instead dips south in this area. This earthquake distribution projects to the sea floor at roughly the location of the MMF, although the two interpretations (Le Pichon et al., 2001, and Armijo et al., 2002) are not precisely in agreement about the location of the MMF in this area.

At eastern end of the MMF, we can recognize three groups of microearthquakes (Fig. 5d). The eastern two groups were located on faults, close to where they bifurcate from the North Anatolian Fault that may be vertical; but further investigations are required to confirm this, due to the limited number of events acquired. On the other hand, this seismicity in the eastern Çınarcık basin does roughly correspond with aftershock activity of the Gölcük–İzmit (Kocaeli) earthquake (Özalaybey et al., 2002) in Armutlu peninsula, though the observed clusters were outside the OBS array.

5. Composite focal mechanisms

Most microearthquakes were too small (M<2) to determine focal mechanism of each event. We therefore attempted to obtain composite focal mechanisms, which were determined by plotting first-motion polarities of P-waves, with a grid-search for possible nodal planes indicating the fault geometry in the region. Composite focal mechanisms may yield reliable information if a rock volume is deforming in response to a uniform regional stress tensor (Zoback, 1992).

These composite focal mechanisms are summarized in Fig. 6 and Table 2. In the western Sea of Marmara, composite focal mechanisms 1 and 2 are located just beneath the MMF and have pure strike-slip focal mechanisms. Mechanism 9 farther east also involves strike-slip. These results suggest that a right-lateral strike-slip stress regime is dominant in this area.

In the Çınarcık Basin, on the other hand, relatively complex mechanisms exist. Our results show a strike-slip type mechanism (No. 3) in its NW part, and a normal-faulting mechanism (No. 4) in its central part. The dip of the south-dipping nodal plane of this normal-faulting mechanism (about 50°) is roughly equal to the local dip of the MMF determined by the earthquake distribution (Fig. 5c). These results suggest that the stress field involves oblique extension to the trend of the MMF in the western Çınarcık Basin.

In the eastern Çınarcık Basin, mechanism 5 involved strike-slip with a small extensional component. As suggested in the previous section, in this most

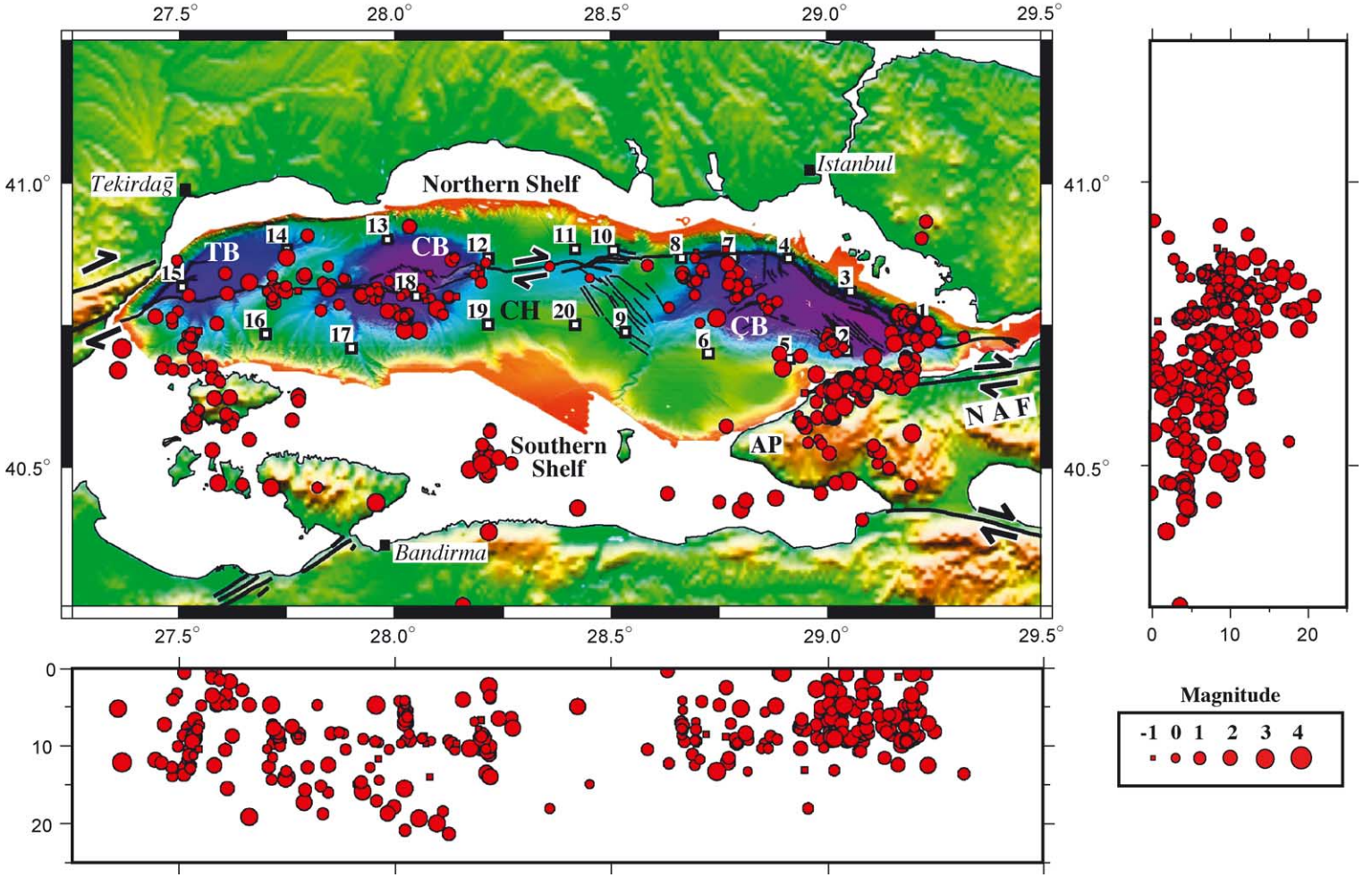

Fig. 4. The distribution of epicenters and hypocenters of microearthquakes determined in this study. See Fig. 1b caption for other details.

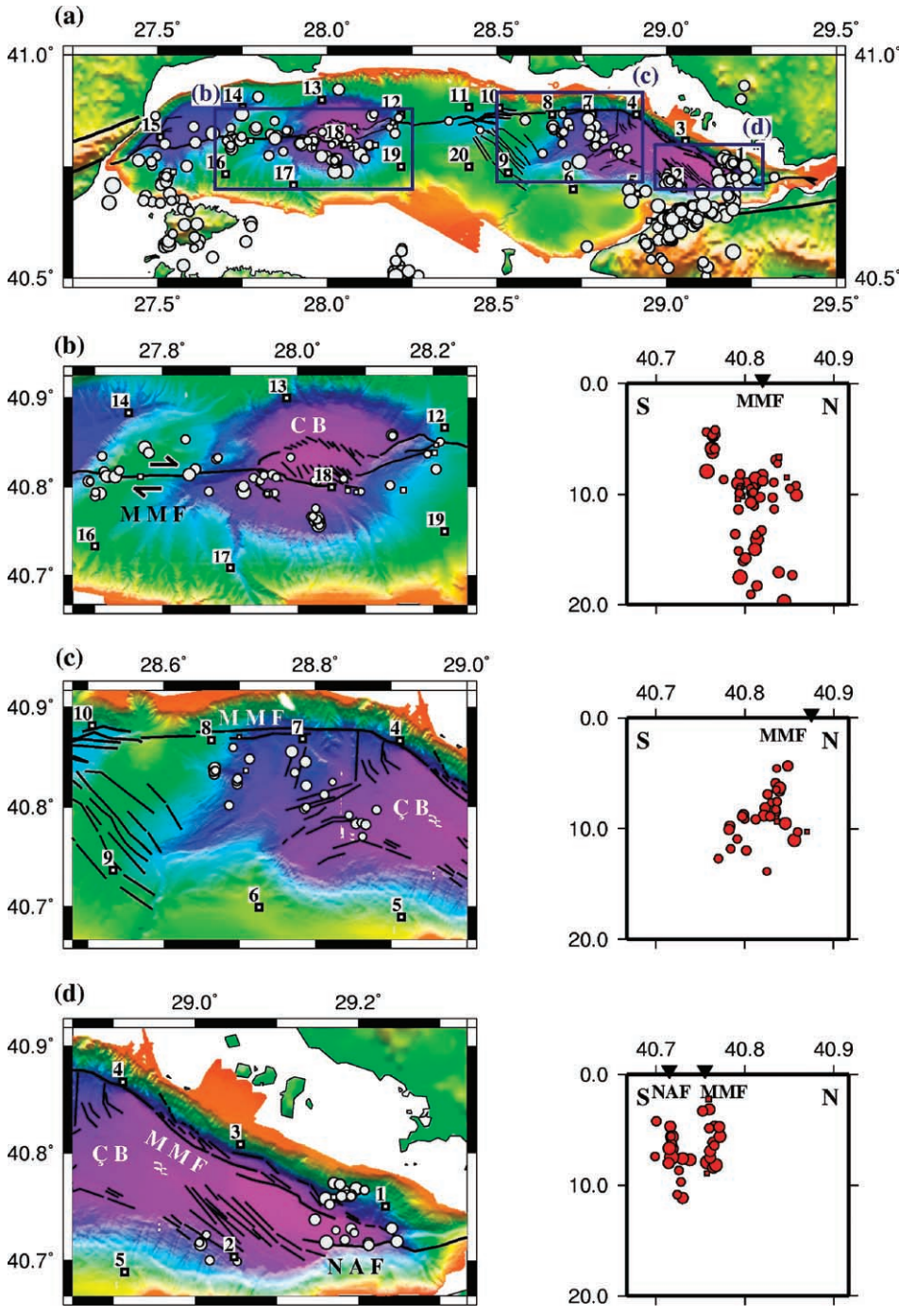

Fig. 5. Relocated epicenter distributions and N–S cross-sections using HypoDD. (a) Map of the selected clusters. Rectangles indicate each selected area. In this map, epicenters determined by HYPOMH are shown. (b) Relocated events in the cluster along the western MMF. (c) Relocated events in the cluster in the western Çınarcık Basin; and (d) relocated events in the cluster at the eastern end of the MMF. Triangles above the cross-sections indicate the surface positions of faults: Main Marmara Fault (MMF), North Anatolian Fault (NAF), Central Basin (CB), Çınarcık Basin (ÇB). For sources of bathymetry data and fault interpretations, see the caption to Fig. 1b.

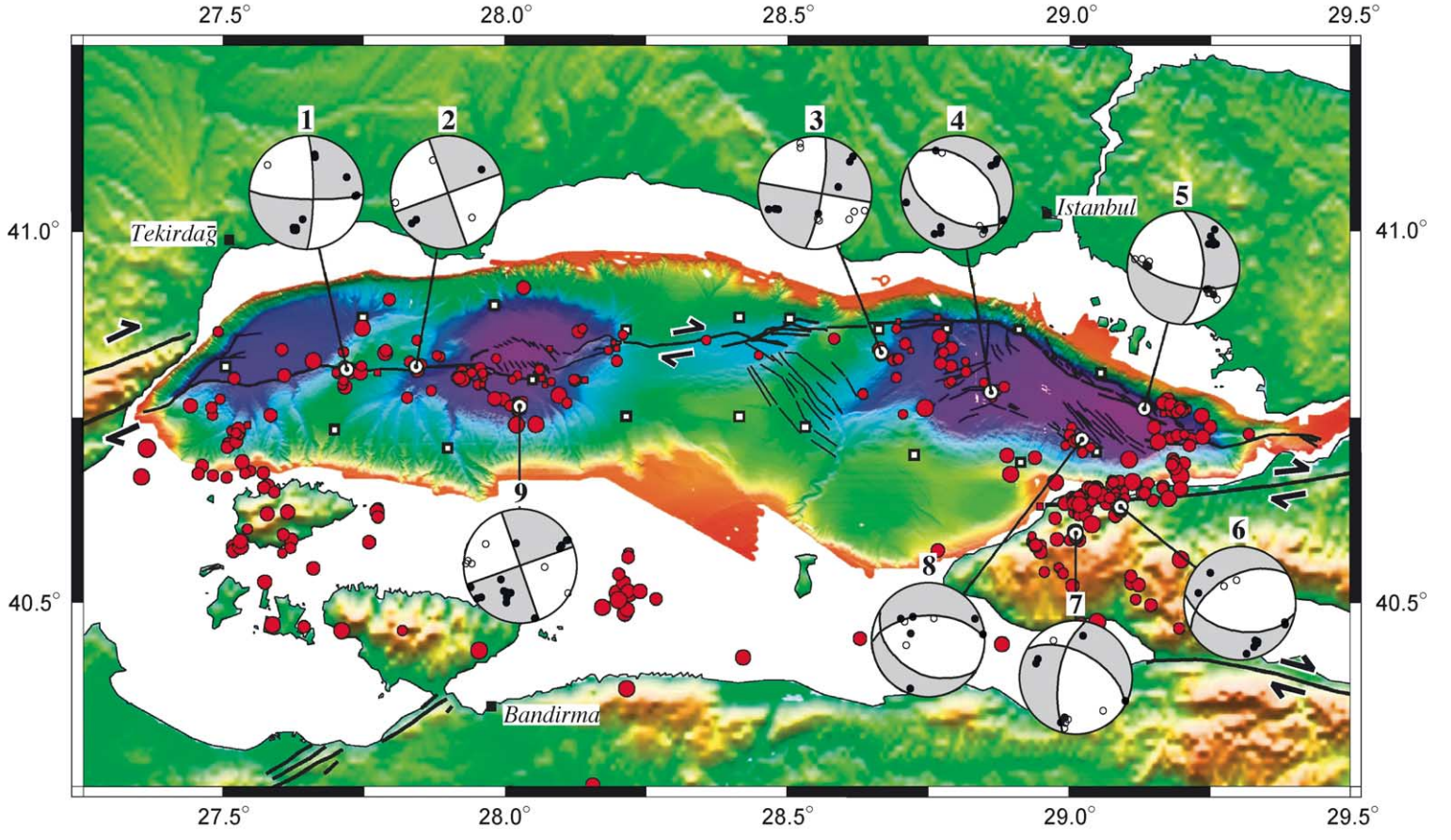

Fig. 6. Composite focal mechanisms, obtained from cluster analyses, represented as equal-area projections on the lower hemisphere. Open circles in each focal mechanism show dilatations; solid circles show compressions. Compressional quadrants are shaded in gray. Bathymetry data and interpretation of the Main Marmara Fault are from the same sources as Fig. 1b.

Table 2
Composite microearthquake focal mechanisms from cluster analyses

Event no.	Number of events	Average latitude (°N)	Average longitude (°E)	Average depth (km)	Strike (°)	Dip (°)	Rake (°)
1	9	40.8131	27.7213	10.1	0	80	−10
2	2	40.8169	27.8441	11.2	70	90	−180
3	8	40.8362	28.6669	7.1	280	90	170
4	3	40.7832	28.8606	10.6	120	50	−100
5	10	40.7606	29.1313	9.6	0	60	−30
6	10	40.6297	29.0901	6.5	240	50	−120
7	9	40.5939	29.0109	9.3	190	65	−40
8	4	40.7201	29.0215	5.3	120	40	−65
9	17	40.7642	28.0273	5.4	70	90	−180

easterly part of this basin the MMF and NAF are subvertical. Mechanism 8 in the south of this basin involved normal faulting with a minor oblique component. The average depth of the microearthquakes that contribute to this composite focal mechanism is shallow, and many normal faults were observed locally in the multibeam survey of IFREMER N/O Le Suroit (bathymetry in Figs. 1b and 4; Le Pichon et al., 2001). Nearby, on Armutlu Peninsula, our results (Nos. 6 and 7) also show normal-faulting mechanisms with minor oblique components. Although the reliability of the mechanisms on this peninsula is relatively low because these are outside the OBS network, our results are consistent with mechanisms determined from land-based observations (Özalaybey et al., 2002). These observations of oblique normal-faulting microearthquakes suggest the presence of strain partitioning in the eastern Çınarcık Basin and Armutlu Peninsula.

This composite focal mechanism analysis supports the view that the western MMF behaves like a single strike-slip fault, but its eastern part reflects more complex deformation. It also confirms that the MMF is subvertical in the western Sea of Marmara, but dips southward in the western part of the Çınarcık Basin.

6. Discussion

We have observed many microearthquakes during the Marmara OBS experiment, which reveal a more detailed earthquake distribution than those observed by land-based observations. In the western Sea of Marmara, most microearthquakes occurred beneath the MMF. Very few occurred along the northern edges of the Central and Tekirdağ Basins and beneath the northern half of the spindle-shaped structure in the Central Basin. From the N–S cross-section (Fig. 5b) and focal mechanisms (events 1, 2, and 9 in Fig. 6), the MMF is locally subvertical and involves pure strike-slip. These observations imply that the MMF is the only active fault in this area. This result supports the single localized active throughgoing right-lateral strike-slip fault system described by Le Pichon et al. (2001) in the western Sea of Marmara.

In contrast, the fault system in the eastern Sea of Marmara is relatively complex. The microearthquake distribution shows that the dip of the MMF is ~45° towards south in the western Çınarcık Basin (Fig. 5c). The composite focal mechanisms in this area may suggest that the average stress field involves oblique extension. These observations further suggest that the western Çınarcık Basin has an oblique extensional regime, as proposed by Armijo et al. (2002).

On the other hand, our results indicate vertical faults at the eastern end of the Çınarcık Basin, with a normal-faulting mechanism in the southern part of this basin. Focal mechanisms of well-located aftershocks of the 1999 earthquake sequence at the northern margin of this basin (Özalaybey et al., 2002) involve almost pure strike-slip. These observations suggest that strain partitioning is occurring within the eastern part of the Çınarcık Basin, as proposed by Le Pichon et al. (2001). Unfortunately, we could not obtain any events along the bending part of the MMF at the northern margin of the central Çınarcık Basin (around OBSs 3 and 4; Figs. 1b and 5c). Thus, we could not reveal the fault

configuration linking the western part (45° southward dip) and the eastern part (vertical) of this basin. On the other hand, the focal mechanism of Çınarcık earthquake (M_s=6.4) of September 18, 1963 (location 40.90°N, 29.20°E by ISC; M_o=96×10^{16} N m, depth 15 km, strike 304°, dip 56°, rake −82° and slip vector azimuth 034° after Taymaz et al., 1991) confirms the existence of normal faulting with a shallow focal depth in this area. Hence, the configuration of the MMF in the middle part of this basin still requires further investigations to better understand the complexity of faulting associated with earthquakes at seismogenic zones.

We also observed many microearthquakes and determined normal-faulting composite focal mechanisms in the northern part of Armutlu Peninsula. These results are consistent with observations of aftershocks of the 1999 Gölcük–İzmit (Kocaeli) earthquake (Taymaz, 2001; Özalaybey et al., 2002; Karabulut et al., 2002). However, the quality of these results is relatively low because these events were located outside the OBS network. To investigate the microseismicity of this area in detail, a combination of the OBS and land-based data will be needed, and will be discussed elsewhere.

7. Conclusions

Microearthquake activity is intense in the eastern Çınarcık Basin and along the proposed trace of the MMF in the middle of the Marmara Sea, its Central and Tekirdağ basins. On the western MMF, most microearthquakes occurred just beneath this fault, and composite focal mechanisms indicate a simple strike-slip regime. These results indicate that the western MMF is subvertical. On the other hand, in the Çınarcık basin (the eastern MMF), many microearthquakes occurred not just beneath the MMF, but also clustered south of it. This microearthquake hypocenter distribution suggests that the eastern MMF dips south at ~45°, and the projected position of this distribution to the sea floor is consistent with the location of the MMF. A composite focal mechanism in this central part of the Çınarcık Basin showed normal faulting with a southward dip of ~50°. These results indicate that the eastern MMF dips southward. Composite focal mechanisms also show a complex stress regime (involving strike-slip and normal faulting) along the eastern Main Marmara Fault (MMF).

Acknowledgements

We are grateful to NATO (grant no: 976744), the Institut de Physique du Globe de Paris, TÜBİTAK, TÜBA and Istanbul Technical University for supporting this Marmara Sea OBS and Land Seismograph Project and for helping us to conduct this experiment following the destructive earthquake of August 17, 1999. We would like to acknowledge the support given by A.M. Celâl Şengör, Xavier Le Pichon, Naci Görür, and Gülsün Sağlamer, and also thank the Hydrographic Department of the Turkish Navy, the captains and crews of Turkish Navy Research Vessel Çubuklu and other boats of the Turkish Navy, the Coastguard, and the mayor of Marmara Island for their professional and effective assistance, which ensured the completion of the cruises under some difficult circumstances and conditions. We also thank Tuğrul Genç, Emin Demirbağ and Argun Kocaoğlu for helping us during deployment and recovery of OBSs. Rob Westaway and anonymous reviewers provided helpful comments on this manuscript. The figures were generated using the GMT software (University of Hawaii; Wessel and Smith, 1998). This work has also been supported by TÜBİTAK–YDABAG projects 100Y082 and 101Y069, and by the Turkish Academy of Sciences (TÜBA), in the framework of their Young Scientist Award Programme (Tuncay Taymaz /TÜBA-GEBİP/2001-2-17).

References

Ambraseys, N.N., Jackson, J.A., 2000. Seismicity of the Sea of Marmara (Turkey) since 1500. Geophys. J. Int. 141, F1–F6.

Armijo, R., Meyer, B., Navarro, S., King, G., Barka, A., 2002. Asymmetric slip partitioning in the Sea of Marmara pull-apart: a clue to propagation processes of the North Anatolian Fault? Terra Nova 14, 80–86.

Barka, A., Kadinsky-Cade, K., 1988. Strike-slip fault geometry in Turkey and its influence on earthquake activity. Tectonics 7, 663–684.

Gürbüz, C., et al., 2000. The seismotectonics of the Marmara region (Turkey): results from a micro-seismic experiment. Tectonophysics 316, 1–17.

Hirata, N., Matsu'ura, M., 1987. Maximum-likelihood estimation of hypocenter with origin time eliminated using nonlinear inversion technique. Phys. Earth Planet. Inter. 47, 50–61.

Hirata, N., Kanazawa, T., Suyehiro, K., Iwasaki, T., Shimamura, H., 1989. Observations of microseismicity in the southern Kuril Trench area by arrays of ocean bottom seismometers. Geophys. J. Int. 98, 55–68.

İmren, C., Le Pichon, X., Rangin, C., Demirbağ, E., Ecevitoğlu, B., Görür, N., 2001. The North Anatolian Fault within the Sea of Marmara: a new interpretation based on multi-channel seismic and multi-beam bathymetry data. Earth Planet. Sci. Lett. 186, 143–158.

Karabulut, H., Bouin, M.P., Bouchon, M., Dietrich, M., Cornou, C., Aktar, M., 2002. The seismicity in the eastern Marmara Sea after the 17 August 1999, İzmit earthquake. Bull. Seismol. Soc. Am. 92, 387–393.

Kasahara, J., Matsubara, T., Sato, T., Koresawa, S., Katao, H., 1995. Development of MOOBS/H (magneto-optical ocean bottom seismometer with hydrophone)-1 (in Japanese with English abstract). J. Mar. Acoust. Soc. Jpn. 22, 45–59.

Le Pichon, X., Şengör, A.M.C., Demirbağ, E., Rangin, C., Imren, C., Armijo, R., Görür, N., Çağatay, N., Mercier de Lepinay, B., Meyer, B., Saatçılar, R., Tok, B., 2001. The main Marmara fault. Earth Planet. Sci. Lett. 192, 595–616.

Okay, A.I., Kaşlılar-Özcan, A., Imren, C., Boztepe-Güney, A., Demirbagı, E., Kuşçu, I., 2000. Active faults and evolving strike-slip basins in the Marmara Sea, northwest Turkey: a multichannel seismic reflection study. Tectonophysics 321, 189–218.

Özalaybey, S., Ergin, M., Aktar, M., Tapırdamaz, C., Biçmen, F., Yörük, A., 2002. The 1999 İzmit earthquake sequence in Turkey: seismological and tectonic aspects. Bull. Seismol. Soc. Am. 92, 376–386.

Rangin, C., Demirbağ, E., İmren, C., Crusson, A., Normand, A., Le Drezen, E., Le Bot, A., 2001. Marine Atlas of the Sea of Marmara. IFREMER-Brest Technology Center, France.

Sato, T., Kasahara, J., Katao, H., Tomiyama, N., Mochizuki, K., Koresawa, S., 1997. Seismic observations at Yap Islands and the northern Yap Trench. Tectonophysics 271, 285–294.

Sato, T., Fujie, G., Koresawa, S., Kasahara, J., Tanaka, K., Honda, S., Yokota, T., Nakamura, K., Naito, H., Ishikawa, Y., Hirasawa, T., 1999. Seismic observations at a seismic gap in the eastern margin of the Japan Sea using ocean bottom seismometers. Tectonophysics 302, 1–7.

Smith, W.H.F., Sandwell, D.T., 1997. Global seafloor topography from satellite altimetry and ship depth soundings. Science 277, 1957–1962.

Smith, A.D., Taymaz, T., Oktay, F., Yüce, H., Alpar, B., Başaran, H., Jackson, J.A., Kara, S., Şimşek, M., 1995. High-resolution seismic profiling in the Sea of Marmara (NW Turkey): late quaternary sedimentation and sea-level changes. Bull. Geol. Soc. Am. 107, 923–936.

Taymaz, T., 1999. Seismotectonics of the Marmara Region: source characteristics of 1999 Gölcük–Sapanca–Düzce earthquakes. Proceedings of ITU-IAHS, International Conference On The Kocaeli Earthquake 17 August 1999, Istanbul-Turkey, 2–5 December 1999, pp. 55–78.

Taymaz, T., 2000. Seismotectonics of the Marmara Region: source parameters of 1999 Gölcük–Sapanca–Düzce earthquakes. NATO Advanced Research Seminar: Integration of Earth Sciences Research on the 1999 Turkish and Greek Earthquakes and Needs for Future Cooperative Research, May 14–17, 2000, Istanbul-Turkey, pp. 26–30. Abstracts Book.

Taymaz, T. (Ed.), 2001. Symposia On Seismotectonics of the North-Western Anatolia-Aegean and Recent Turkish Earthquakes, Scientific Activities 2001, Istanbul Technical University, Faculty of Mines, May 8, 2001, Istanbul, TurkeyISBN: 975-97518-0-1. 113 pp.

Taymaz, T., Jackson, J.A., McKenzie, D., 1991. Active tectonics of the North and Central Aegean Sea. Geophys. J. Int. 106, 433–490.

Taymaz, T., Kasahara, J., Hirn, A., Sato, T., 2001. Investigations of micro-earthquake activity within the Sea of Marmara and surrounding regions by using Ocean Bottom Seismometers (OBS) and land seismographs: initial results. Scientific Activities 2001 Symposia Book, pp. 42–51. Istanbul Technical University, Faculty of Mines, May 8, 2001, Istanbul, Turkey. ISBN: 975-97518-0-1. 113 pages.

Taymaz, T., Sato, T., Kasahara, J., Hirn, A., Ito, M., Kamimura, A., Hayakawa, T., Tan, O., 2002. Investigations of micro-earthquake activity within the Sea of Marmara and surrounding regions by using ocean bottom seismometers (OBS) and land seismographs: final results. 1st International Symposium of Istanbul Technical University the Faculty of Mines on Earth Sciences and Engineering, 16–18 May 2002, Istanbul, Turkey, p. 53. Abstracts Book: SS-B-Oral.

Tsumura, K., 1967. Determination of earthquake magnitude from total duration of oscillation. Bull. Earthq. Res. Inst. Univ. Tokyo 45, 7–18.

Waldhauser, F., 2001. HypoDD: a program to compute double-difference hypocenter locations. U.S. Geol. Survey Open-file report, 01-113, Menlo Park, California.

Waldhauser, F., Ellsworth, W.L., 2000. A double-difference earthquake location algorithm: method and application to the northern Hayward fault, California. Bull. Seismol. Soc. Am. 90, 1353–1368.

Wessel, P., Smith, W.H.F., 1998. New improved version of Generic Mapping Tools released. EOS Trans.-AGU 79, 579.

Zoback, M.L., 1992. First-and second-order patterns of stress in the lithosphere: the world stress map project. J. Geophys. Res. 97, 11703–11728.